ChemSystemsChem

Research Article
doi.org/10.1002/syst.202200008

Chemistry Europe
European Chemical Societies Publishing

www.chemsystemschem.org

Controlling Self-Sorting versus Co-assembly in Supramolecular Gels

Santanu Panja,[a] Bart Dietrich,[a] Andrew J. Smith,[b] Annela Seddon,[c, d] and Dave J. Adams*[a]

Supramolecular gels formed by the combination of different organic molecules are of significant interest in the search of new functional materials. When two different molecules are mixed to form gels, the self-assembled fibres can be a result of self-sorting or co-assembly. A key challenge is to control the network type. Here, we demonstrate that control over the network type can be achieved either by varying the hydrophobicity of a component or by employing a pH-switch method.

Introduction

In supramolecular gels, small organic molecules (called gelators) interact noncovalently to form a fibrous network which immobilizes the solvent. The gel network is maintained by noncovalent interactions and so the self-assembled gels are dynamic in nature and exhibit excellent responsiveness when exposed to stimuli like heat, pH, UV-light, ionic analytes etc.[1] This responsive behaviour enables accessing of materials with various properties from a single gelator building block.

An alternative strategy to adapt gel properties is to incorporate two or more components during self-assembly.[2] Such multicomponent systems are receiving interest because of their widespread application and advantages over single-component systems. For instance, mixing different components can lead to various complex structures, diverse morphologies and tunable properties that are hard to achieve with any of the single components.[2b,3] The molecular homogeneity of single component gels can be altered by multicomponent self-assembly which enables material exploration for drug delivery, nanoreactor design, tissue engineering and optoelectronics.[2b,4]

Gelation from individual molecules occurs through a multi-level self-assembly process. Initially, phase separation happens which allows the molecules to self-assemble into one-dimensional fibres. Subsequent entanglement or crosslinking of these fibres results in the hydrogel network. When two different components are present, they may undergo phase separation independently or together. Independent phase separation of the components leads to self-sorted gel networks where pure assemblies of one component coexist with pure assemblies of the other. Both types of assemblies then contribute to form the matrix.[5] In contrary, co-assembly results in fibres comprising of both components.[5] A mixture of self-sorting and co-assembly is also possible.[5] However, many factors such as chirality, hydrogen bonding complementarity, steric effects, kinetic and thermodynamic pathway control etc. can promote one particular type of assembly over the other.[6]

One method for preparing multicomponent gels is to combine a gelator with a non-gelling organic compound.[3,7] In such systems, the gel matrix can be a result of self-sorting of the gelator while the additive strongly influences the nucleation and growth of the fibres (i.e., the microstructure), and thereby controls the bulk properties (Figure 1).[3,7] It has also been reported that, if the non-gelling additive and the gelator component have similar molecular structure, mixing of the components results in co-assembly as opposed to a self-sorted system.[8] Here we show that combination of a dipeptide gelator (compound **1**) with non-gelling amphiphiles (compounds **2**–**6**) can produce gels at low pH whilst the properties of the multicomponent systems are significantly dependent on the hydrophobicity of the non-gelling component (Figure 1). We have previously shown that Fmoc-amphiphiles with short alkyl chain (compounds **2**–**4**) primarily undergo self-sorting with **1**.[9] Here, we find that, when the amphiphiles are more hydrophobic (**5** and **6**), gel formation is driven by co-assembly. Importantly, the assembly pattern in the multicomponent systems can be altered by changing the preparative pathway (Figure 1). Instead of direct mixing, a pH switch method is employed that alters the assembly pattern from self-sorting to co-assembly (or vice versa). As such, we are able to control the network type as well as material properties either by varying hydrophobicity or by changing the preparative pathway.

[a] Dr. S. Panja, Dr. B. Dietrich, Prof. D. J. Adams
School of Chemistry, University of Glasgow
Glasgow, G12 8QQ (U.K)
E-mail: dave.adams@glasgow.ac.uk
[b] Dr. A. J. Smith
Diamond Light Source Ltd., Diamond House
Harwell Science and Innovation Campus
Didcot, Oxfordshire OX11 0DE (U.K.)
[c] Dr. A. Seddon
School of Physics, HH Wills Physics Laboratory
University of Bristol, Tyndall Avenue, Bristol, BS8 1TL (U.K.)
[d] Dr. A. Seddon
Bristol Centre for Functional Nanomaterials
HH Wills Physics Laboratory, University of Bristol
Tyndall Avenue, Bristol, BS8 1TL (U.K.)

Supporting information for this article is available on the WWW under https://doi.org/10.1002/syst.202200008

© 2022 The Authors. ChemSystemsChem published by Wiley-VCH GmbH. This is an open access article under the terms of the Creative Commons Attribution License, which permits use, distribution and reproduction in any medium, provided the original work is properly cited.

© 2022 The Authors. ChemSystemsChem published by Wiley-VCH GmbH

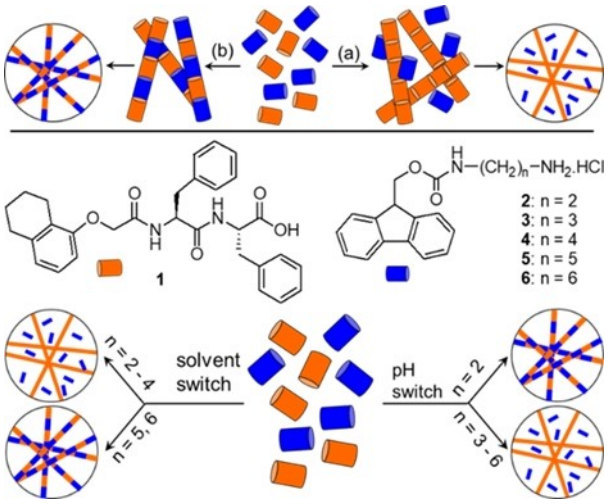

Figure 1. Top: cartoon schematic showing how the assembly of a binary system comprising of a gelator (orange) and a non-gelling compound (blue) can lead to (a) self-sorting and (b) co-assembly during gelation. Bottom: Chemical structures of compounds **1**–**6** used in the study. Depending on the preparative pathway, the hydrophobicity of the non-gelling Fmoc-salts determines the assembly patterns in the multicomponent gels of **1** with **2**–**6**.

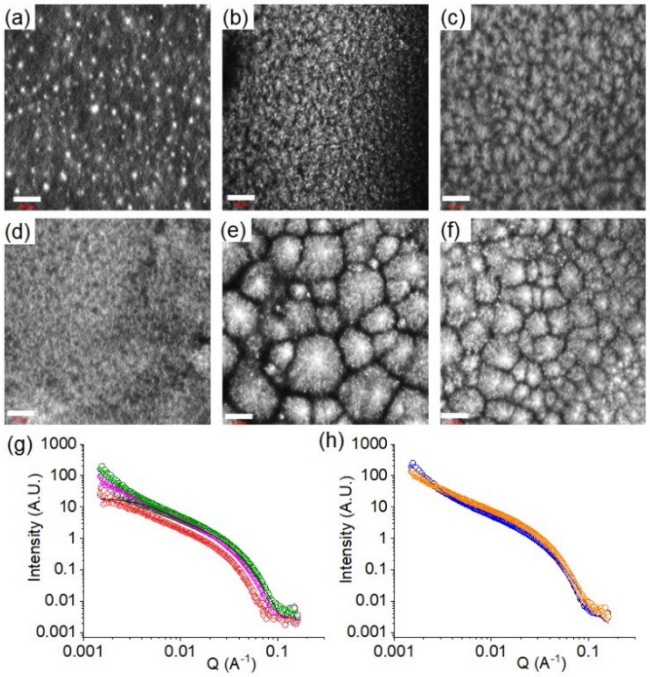

Figure 2. Confocal fluorescence microscopy images (scale bars represent 20 μm) of (a) the hydrogel of **1** and (b–f) the multicomponent gels of **1** with **2**–**6** respectively. (g) SAXS data for the hydrogel of **1** (black) and the multicomponent gels of **1** with **2** (red), **3** (magenta) and **4** (green). (h) SAXS data for the multicomponent gels of **1** with **5** (blue) and **6** (orange). In all cases, the open circles show the data, and the lines are the fits to the data. For (a–h), concentrations of **1**–**6** are 2 mg/mL, solvent is DMSO/H2O (20/80, v/v).

Results and Discussion

Dipeptide **1** forms a self-supported, invertible gel almost instantly (within few seconds) in DMSO/H_2O (20/80, v/v) (Figure 1, bottom).[9] The pH of the gel is around 4.3. The hydrogel network consists of spherulitic domains of fibres as can be seen from confocal microscopy imaging (Figure 2a). Under similar conditions, compounds **2**–**6** produce free flowing solutions with pH in the range 4.9–5.3 (Figure S2). Fluorescence studies confirm that all the compounds **2**–**6** exist in their respective monomeric form in solution exhibiting emission at 318 nm with almost equal intensity (Figure S3).[10] Combination of **1** and **2**–**6** individually results a gel in all cases with a pH of 3.1–3.3 (Figure S4). In the multicomponent gels, the ratios of the components were kept the same as optimised in a previous study.[9] Despite the nonaggregation tendency of compounds **2**–**6** in solution, the microstructure and mechanical properties of the multicomponent gels were very dependent on the hydrophobicity of the Fmoc-amphiphiles. As previously described,[9] the multicomponent gels of **1** with **2**–**4** exhibit spherulitic domains of fibres in their microstructure, very similar to the hydrogel of **1** alone (Figure 2). However, the multicomponent gels contain a higher density of spherulitic nucleation centres. We previously suggested that the increase in density of spherulitic structures in the multicomponent gels is due to salt effects arising from the hydrochloride salts **2**–**4**.[9] The presence of the salts can affect the structuring of the underlying peptide network involving the Hofmeister effect.[11]

Moving to the multicomponent gels of (**1** + **5**) and (**1** + **6**), a dramatic change in the microstructure was noticed. In both cases, the underlying network consisted of large spherulitic domains of fibres (Figure 2). Hydrogels with identical microstructure exhibit similar rheological properties (Figure S5–S7). We have shown that the rheological moduli (the storage and loss moduli, G′ and G″) for the multicomponent gels of (**1** + **2**) to (**1** + **4**) and the hydrogel of **1** alone were almost the same.[9] There was no substantial change in the strain bearing capacity (critical strain or gel strength is 6–8%) of the gels either. In contrast, the stiffness (G′) as well as gel strength gradually increases for the systems (**1** + **5**) and (**1** + **6**) (Figure S5–S7). These results suggest that in the multicomponent gels of **1** with **2**–**4**, the fibre formation was driven primarily by the self-sorting of **1** whilst compounds **2**–**4** behave as non-gelling additives.[7,9] When the cationic salts are more hydrophobic (**5** and **6**), the gel fibres are formed from both the components resulting in co-assembly. The results resemble the systems reported by the Ulijn group, who showed that in the presence of hydrophobic non-gelling amphiphiles gelators undergo co-assembly as opposed to self-sorting.[8b]

Spectroscopic studies were conducted on the gels to infer the molecular level interactions.[5] We have reported that **1** in its gel state adopts a β-sheet conformation with the appearance of a strong band at 1648 cm^{-1} in FTIR corresponding to the stretching of the hydrogen bonded amide carbonyls (Figure S8, S9).[9] Simultaneous emergence of a shoulder peak (minor) at 1687 cm^{-1} indicates that the peptide is arranged in an antiparallel fashion.[9] In the mixed gels, this shoulder peak overlaps with the carbamate carbonyls of **2**–**6** and appears at 1681 cm^{-1}. The carboxylic –OH of **1**, the amide and carbamate

© 2022 The Authors. ChemSystemsChem published by Wiley-VCH GmbH

-NHs of **1** and **2**–**6** respectively, all became too broad to distinguish in the multicomponent gels. For all of the multicomponent systems, the amide –C=O stretching appeared at ~1647 cm^{-1} indicating establishment of the antiparallel β-sheet structures in the mixed systems.[12] Interestingly, the multicomponent gels of (**1** + **5**) and (**1** + **6**) additionally showed a new peak at 1643 cm^{-1} signifying a difference in the hydrogen bonded networks.[13] Moreover, by fluorescence, while the multicomponent gels of (**1** + **2**) to (**1** + **4**) exhibited identical emission characteristics with a strong emission at 320 nm, the binary gels (**1** + **5**) and (**1** + **6**) showed 2 nm red shifts in emission spectra (Figure S10). These data suggest a change in the underlying molecular packing of the gels (**1** + **5**) and (**1** + **6**) from the rest of the multicomponent systems.

The results further intimate that the changes in underlying molecular packing with increase in hydrophobicity of the Fmoc-amphiphiles may be subtle, but hugely influence the fibre level assembly and their distribution on longer length scales, i.e., the microstructure of the gels, and consequently the bulk properties.[5] This was further supported by small angle X-ray scattering (SAXS) data. The SAXS data for the hydrogel of **1** fit well to a flexible elliptical cylinder model with a radius of 3.3 nm and an axis ratio of 2 (Figure S11, Table S1). In contrast, the data for the individual components **2**–**6** fit to a power law only suggesting a lack of significant assembly. For the multicomponent gels, the scattering patterns are very similar and fit to either a flexible elliptical cylinder (for **1** with **2**, **3**, and **6**) or a flexible elliptical cylinder with a power law (**1** with **4** and **5**) (Figure S12, Table S2). Of the different multicomponent systems, while the hydrogel (**1** + **2**) showed a larger radius of 4.2 nm with the same axis ratio of 2 as of **1**, the rest of the binary gels exhibited comparable radius within the range 3.1–3.5 nm with axis ratio of 1.5–2.5. This implies that the primary self-assembled structures are similar for the gels. However, there are differences in the distribution and crosslinking of the fibres at longer length scales i.e., the microstructure of the gels as realized by confocal microscopy which influences the bulk material properties.

Instead of direct mixing of the components, we next employed a pH switch method to control the assembly type of the multicomponent gels (Figure 1, bottom). We have reported that a slow pH-decrease can lead to self-sorting in multicomponent peptide systems instead of co-assembly through sequential assembly of the peptides subjected to their pK_a.[6f] However, in the present case, instead of a solution at high pH, mixtures of **1** with **2**–**6** individually resulted in gel in all cases (pH 10.2–10.4) (Figure S13). Compounds **2**–**6** were stable under these (Figure S14).[14] None of the components **1**–**6** has gelling ability on their own at high pH in DMSO/H_2O (20/80, v/v). Above the pK_a of **1** (pK_a of **1** is 6.4, Figure S15),[9] the corresponding carboxylate anion is unable to maintain the gel structure due to electrostatic repulsion and produces a sol. Deprotonation of the terminal ammonium functionality at a pH above the pK_a of **2**–**6** (pK_a of **2**–**6** is calculated to be in the range 8.6–9.1, Figure S15) resulted in formation of corresponding amine. While the amine form of **2** remained in solution, compounds **3**–**6** in their respective deprotonated state produced precipitation. Hence, the multicomponent gelation of **1** with **2**–**6** at high pH is purely driven by co-assembly.

We used the hydrolysis of glucono-δ-lactone (GdL) to gluconic acid which reduces the pH.[15] Correlation of the pH-time profile with time sweep rheology following the storage and loss moduli (G′ and G″ respectively) for **1** alone (Figure 3a) shows that gelation begins (G′ > G″) at a pH below the pK_a of **1**. Over time, the rheological moduli gradually increase as assembly proceeds and become almost constant after 13 hours. Analysis of tanδ (G″/G′) further correlates gradual conversion of a free-flowing solution into a gel with the pH decrease over time (final pH 4.2–4.3). The SAXS data for the gel fit to a flexible elliptical cylinder model with a radius of 2.9 nm and an axis ratio of 5.9 (Figure S16, Table S3).

When adding GdL to the multicomponent systems (**1** + **2**) to (**1** + **6**) in presence of base, no significant change in rate of pH decrease was noticed (Figure 3b, Figure S17). However, the main difference was observed in the rheology. For all the multicomponent systems, the initial values of G′ were considerably higher than G″ indicating that a gel was being formed even before the measurement could begin (Figure 3b, Figure S17). The rheological moduli evolve with time critically maintaining a gel state throughout the process (final pH of the gels is 4.0–4.1) (Figure S18). The tanδ values recorded over time confirm gradual increase in solid-like nature of the gel (higher G′) with the pH decrease (Figure 3b, Figure S17).

Oscillatory strain and frequency sweeps were conducted to evaluate the mechanical properties of the gels obtained by the pH-switch (Figure S19–S21). All the multicomponent gels exhibited lower stiffness than hydrogel of **1** alone. Interestingly, the multicomponent gels of (**1** + **3**) to (**1** + **6**) exhibit identical mechanical properties in rheology. These gels have almost equal stiffness (G′) and strain bearing capacity (critical strain is 4–6%). In comparison, ~50% reduction in gel stiffness was realized for the gel (**1** + **2**). While the binary systems (**1** + **3**) to (**1** + **6**) exhibit densely packed long fibres similar to the gel of **1** alone, the multicomponent gel of (**1** + **2**) showed large spherulitic domains of fibres as its microstructure (Figure 4). Multicomponent gels having similar microstructure and rheological properties exhibit identical emission profiles. All the gels (**1** + **3**) to (**1** + **6**) showed a sharp emission peak at 321 nm (Figure S22). In comparison, a red shifted band at 327 nm along with significant broadening at 365 nm was noticed for the

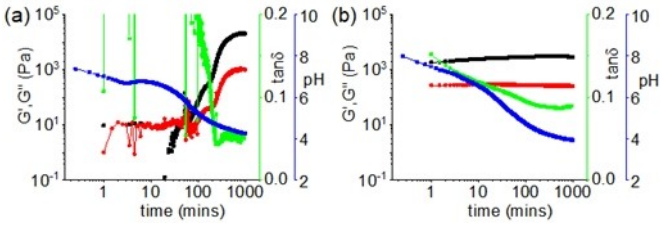

Figure 3. Variation of pH (blue), G′ (black), G″ (red) and tanδ (green) with time for (a) **1** and (b) the mixture of **1** and **2** in presence of GdL. For both systems, initial concentration of NaOH and GdL are 0.01 M and 6 mg/mL, respectively. Initial concentrations of **1** (a, b) and **2** (for b) are 2 mg/mL. Solvent is DMSO/H_2O (20/80, v/v).

© 2022 The Authors. ChemSystemsChem published by Wiley-VCH GmbH

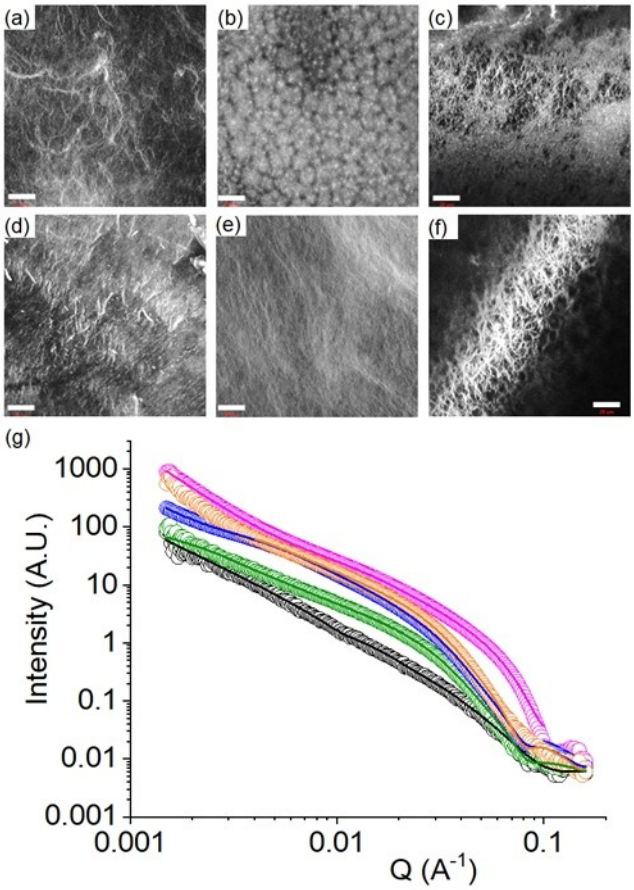

Figure 4. Confocal fluorescence microscopy images (scale bars represent 20 μm) of (a) the hydrogel of **1** and (b–f) the multicomponent gels of **1** with **2**–**6** respectively prepared by the hydrolysis of GdL. (g) SAXS data for the hydrogel of **1** (black) and the multicomponent gels of **1** with **2** (magenta), **3** (green), **4** (blue) and **5** (orange) obtained by the hydrolysis of GdL. In all cases, the open circles show the data, and the lines are the fits to the data. For (a–g), initial concentration of NaOH and GdL are 0.01 M and 6 mg/mL, respectively. Initial concentration of **1** (a–g) is 2 mg/mL and initial concentrations of **2**–**6** (b–g) are 2 mg/mL, solvent is DMSO/H_2O (20/80, v/v).

hydrogel of (**1** + **2**) (Figure S22). Typically, the compounds **2**–**6** exhibit excimer emission in solution at high pH in the region 400–500 nm due to overlapping of the fluorenyl groups in antiparallel fashion (Figure S13, S23).[10,13]

However, the cationic salts can form micellar structures at high concentration and exhibit emission near 365 nm corresponding to the parallel overlapping of the fluorenyl moieties.[16] To verify this, a concentration variable emission study of **2** was conducted that showed appearance of a broad band near 365 nm on or above the concentration of 5 mg/mL (Figure S24). Hence, at low concentration (2 mg/mL), the cationic forms of **2**–**6** primarily exist in monomeric structures in solution and so there was neither any micellar aggregation nor excimer formation at low pH (as indicated by fluorescence and SAXS data, Figure S2, S3 and S11).[9]

In the present study, during gel-to-gel transitions, no emission in the range 400–500 nm was recorded for the mixed systems (Figure S25). However, the final gel of (**1** + **2**) exhibits broadening near 365 nm which is likely due to less efficient aromatic stacking in parallel arrangement of the fluorenyl moieties (Figure S22, S25).[13,16] Such a band was absent in the rest of the multicomponent gels. The different behaviour of **2** with respect to **3**–**6** in the mixed systems is presumably due to short hydrophobic spacer/linker which allows little aromatic stacking at acidic pH. Fmoc-amphiphiles with long hydrophobic spacer are unable to form any excimers probably due to increased flexibility and therefore decreased molecular rigidity.[13] Furthermore, comparison of emission spectra of the gels undoubtedly confirms that only compound **2** is incorporated into the gel fibres (co-assembly formation) (Figure 1). Compounds **3**–**6** act as non-gelling additives but affect the self-sorting of **1**. Interestingly, the scattering patterns are similar for the multicomponent gels (**1** + **3**) to (**1** + **6**) to that of **1** alone exhibiting flexible elliptical cylinder structures (a power law is needed for **1** + **4**, suggesting large scale structure that cannot be resolved from these data) but with a slightly larger radius than **1** (Figure 4g, Figure S16, Table S3). The multicomponent gels (**1** + **3**) to (**1** + **6**) exhibited a comparable radius of 3.9–4.3 nm and an axis ratio of 2.1–2.2, corroborating that the primary assembled structures are identical for these gels. In contrast, the data for the gel of (**1** + **2**) fit to a flexible cylinder model combined with a power law and undoubtedly differ from that of other gels. The fit to the data implies that the cylinders have a radius of 3.7 nm and a length of 76.1 nm significantly shorter than other multicomponent gels. Moreover, high scattering intensity for the (**1** + **2**) gel than other binary gels clearly demonstrate a difference in packing leading to a change in the self-assembled structures. There was also a difference in the FTIR spectrum of the (**1** + **2**) gel to that of the other multicomponent systems. In the gel of (**1** + **2**), the amide and carbamate -NH bending peaks overlap and appeared as a sharp signal at 1584 cm^{-1}.[17] The bifurcation of the peak (appearing at 1597 cm^{-1} and 1584 cm^{-1}) in the gels (**1** + **3**) to (**1** + **6**) signifies a difference in the molecular level packing of the gels (Figure S26). However, all the multicomponent gels exhibit similar absorption characteristics in UV-vis (Figure S27).

Conclusion

In conclusion, we have shown that the network type (i.e., self-sorting or co-assembly) in multicomponent hydrogels comprising of a gelator and a non-gelling amphiphile can be controlled either by increasing hydrophobicity of the non-gelling component or by employing a pH switch method. When the gels are prepared directly, relatively hydrophilic amphiphiles barely affect the self-sorting of the gelator. Non-gelators with long hydrophobic segments tend to lead to co-assembly. On the contrary, when the gelation is triggered by a pH switch method, the assembly pattern is altered. In this case, the non-gelator with a short hydrophobic linker co-assembles with the gelator molecules. The properties of supramolecular gels depend on the preparative pathway.[18] The hydrophobic spacer of the non-gelling amphiphiles clearly dictates the self-assembly kinetics of the multicomponent systems under a given set of conditions.

© 2022 The Authors. ChemSystemsChem published by Wiley-VCH GmbH

As such, we are able to control the network type as well as material properties either by varying hydrophobicity or by changing preparative pathway.

Acknowledgements

SP thanks the University of Glasgow for funding. This work was carried out with the support of Diamond Light Source, instrument I22 (proposal SM27906).

Conflict of Interest

The authors declare no conflict of interest.

Data Availability Statement

The data that support the findings of this study are available in the supplementary material of this article.

Keywords: supramolecular gel · self-sorting · so-assembly · pathway dependence · SAXS · rheology

[1] a) X. Du, J. Zhou, J. Shi, B. Xu, *Chem. Rev.* **2015**, *115*, 13165–13307; b) S. Panja, D. J. Adams, *Chem. Soc. Rev.* **2021**, *50*, 5165–5200.
[2] a) C.-W. Chu, C. A. Schalley, *Org. Mater.* **2021**, *3*, 25–40;b) B. O. Okesola, A. Mata, *Chem. Soc. Rev.* **2018**, *47*, 3721–3736; c) D. M. Raymond, B. L. Nilsson, *Chem. Soc. Rev.* **2018**, *47*, 3659–3720.
[3] L. Li, R. Sun, R. Zheng, *Mater. Des.* **2021**, *197*, 109209.
[4] H. K. Lau, K. L. Kiick, *Biomacromolecules* **2015**, *16*, 28–42.
[5] E. R. Draper, D. J. Adams, *Chem. Soc. Rev.* **2018**, *47*, 3395–3405.
[6] a) A. R. Hirst, B. Huang, V. Castelletto, I. W. Hamley, D. K. Smith, *Chem. Eur. J.* **2007**, *13*, 2180–2188; b) Z. Yu, F. Tantakitti, T. Yu, L. C. Palmer, G. C. Schatz, S. I. Stupp, *Science* **2016**, *351*, 497–502; c) S. Onogi, H. Shigemitsu, T. Yoshii, T. Tanida, M. Ikeda, R. Kubota, I. Hamachi, *Nat. Chem.* **2016**, *8*, 743–752; d) Y. Ma, S. V. Kolotuchin, S. C. Zimmerman, *J. Am. Chem. Soc.* **2002**, *124*, 13757–13769; e) K. Aratsu, R. Takeya, B. R. Pauw, M. J. Hollamby, Y. Kitamoto, N. Shimizu, H. Takagi, R. Haruki, S.-I. Adachi, S. Yagai, *Nat. Commun.* **2020**, *11*, 1623; f) K. L. Morris, L. Chen, J. Raeburn, O. R. Sellick, P. Cotanda, A. Paul, P. C. Griffiths, S. M. King, R. K. O'Reilly, L. C. Serpell, D. J. Adams, *Nat. Commun.* **2013**, *4*, 1480; g) A. Sarkar, R. Sasmal, C. Empereur-mot, D. Bochicchio, S. V. K. Kompella, K. Sharma, S. Dhiman, B. Sundaram, S. S. Agasti, G. M. Pavan, S. J. George, *J. Am. Chem. Soc.* **2020**, *142*, 7606–7617; h) D. J. Cornwell, O. J. Daubney, D. K. Smith, *J. Am. Chem. Soc.* **2015**, *137*, 15486–15492.
[7] L. E. Buerkle, S. J. Rowan, *Chem. Soc. Rev.* **2012**, *41*, 6089–6102.
[8] a) C. Colquhoun, E. R. Draper, E. G. B. Eden, B. N. Cattoz, K. L. Morris, L. Chen, T. O. McDonald, A. E. Terry, P. C. Griffiths, L. C. Serpell, D. J. Adams, *Nanoscale* **2014**, *6*, 13719–13725; b) S. Fleming, S. Debnath, P. W. J. M. Frederix, N. T. Hunt, R. V. Ulijn, *Biomacromolecules* **2014**, *15*, 1171–1184.
[9] S. Panja, B. Dietrich, A. Zydel, A. Trabold, A. Qadir, D. Adams, *Chem. Commun.* **2021**, *57*, 7898–7901.
[10] S. Debnath, S. Roy, Y. M. Abul-Haija, P. W. J. M. Frederix, S. M. Ramalhete, A. R. Hirst, N. Javid, N. T. Hunt, S. M. Kelly, J. Angulo, Y. Z. Khimyak, R. V. Ulijn, *Chem. Eur. J.* **2019**, *25*, 7881–7887.
[11] S. Roy, N. Javid, J. Sefcik, P. J. Halling, R. V. Ulijn, *Langmuir* **2012**, *28*, 16664–16670.
[12] a) C. Tang, A. M. Smith, R. F. Collins, R. V. Ulijn, A. Saiani, *Langmuir* **2009**, *25*, 9447–9453; b) A. M. Smith, R. J. Williams, C. Tang, P. Coppo, R. F. Collins, M. L. Turner, A. Saiani, R. V. Ulijn, *Adv. Mater.* **2008**, *20*, 37–41.
[13] S. Fleming, S. Debnath, P. W. J. M. Frederix, T. Tuttle, R. V. Ulijn, *Chem. Commun.* **2013**, *49*, 10587–10589.
[14] S. Panja, D. J. Adams, *Chem. Commun.* **2019**, *55*, 47–50.
[15] a) D. J. Adams, M. F. Butler, W. J. Frith, M. Kirkland, L. Mullen, P. Sanderson, *Soft Matter* **2009**, *5*, 1856–1862; b) Y. Pocker, E. Green, *J. Am. Chem. Soc.* **1973**, *95*, 113–119.
[16] J. W. Sadownik, J. Leckie, R. V. Ulijn, *Chem. Commun.* **2011**, *47*, 728–730.
[17] a) J. D. Tang, C. Mura, K. J. Lampe, *J. Am. Chem. Soc.* **2019**, *141*, 4886–4899; b) K. Gayen, N. Nandi, K. S. Das, D. Hermida-Merino, I. W. Hamley, A. Banerjee, *Soft Matter* **2020**, *16*, 10106–10114.
[18] J. Raeburn, A. Zamith Cardoso, D. J. Adams, *Chem. Soc. Rev.* **2013**, *42*, 5143–5156.

Manuscript received: February 24, 2022
Accepted manuscript online: March 28, 2022
Version of record online: April 14, 2022

© 2022 The Authors. ChemSystemsChem published by Wiley-VCH GmbH